Upper limit on the isovector parity-violating decay width of the 0^+ $T=1$ state of ^{6}Li

R. G. H. Robertson,* P. Dyer,* and R. C. Melin†
Cyclotron Laboratory and Physics Department, Michigan State University, East Lansing, Michigan 48824

T. J. Bowles*
Physics Division, Argonne National Laboratory, Argonne, Illinois 60439
and Physics Division, Los Alamos National Laboratory, Los Alamos, New Mexico 87545

A. B. McDonald,‡ G. C. Ball, W. G. Davies, and E. D. Earle
Atomic Energy of Canada Limited, Chalk River Nuclear Laboratories, Chalk River, Ontario, Canada K0J 1J0
(Received 27 October 1983)

A search has been made for a resonance in the ^{2}H$(\alpha,\gamma)^6$Li capture-reaction cross section at the energy corresponding to the 0^+, $T=1$, 3.56-MeV state of ^{6}Li. None was found, and an upper limit of 6.5×10^{-7} eV was set on the parity-forbidden α width at the 90% confidence level. This limit is three orders of magnitude smaller than the best previous measurement.

I. INTRODUCTION

The development of unified theories of the weak and electromagnetic interactions, and the consequent prediction of the weak neutral current, leads one to expect that a neutral current will act between hadrons. Finding experimental evidence for this has proven to be exceptionally difficult. In an isospin decomposition of the effective parity-violating nucleon-nucleon force, the $\Delta T=1$ component has special significance because it is particularly sensitive to neutral currents. Recently it has been shown[1-3] that measurements[4,5] in ^{19}F and ^{21}Ne can be analyzed to give a value for the weak πNN coupling constant f_π that dominates isovector parity violation in these cases and originates mainly in neutral currents. In addition, statistically significant evidence for $\Delta T=1$ parity violation has been reported[6,7] for levels in ^{20}Ne. However, the nuclear-structure calculations[8,9] (particularly for ^{20}Ne and ^{21}Ne) are difficult, and the desirability of observing $\Delta T=1$ parity violation in a simpler system has long been recognized.

Four such cases have received experimental and theoretical attention: the capture of polarized neutrons by protons,[10] mixing[11] between the $(J^\pi,T)=(2^-,0)$ and the $(2^+,1)$ states of ^{10}B, mixing[12] between $(0^-,0)$ and $(0^+,1)$ states in ^{18}F, and the parity-violating α decay of the $(0^+,1)$ state at 3.56 MeV in ^{6}Li. In no case has $\Delta T=1$ parity violation been observed, and the best limit comes from ^{18}F (the limit is consistent with the value[2] for f_π obtained from ^{19}F and ^{21}Ne). We report here on a search for resonant α capture by deuterium at the energy of the 3.56-MeV state, which gives a limit on the α width of that state.

TABLE I. Experimental data on $\Gamma_{\alpha d}$ of the 3.56-MeV state of ^{6}Li.

Author	Reference	$\Gamma_{\alpha d}$ (eV)
Wilkinson	13	≤ 0.2
Wahl	18	<0.25
Rasmussen and Swann	19	<1.3
Artemov *et al.*	20	<0.2
Barrette *et al.*	15	≤ 0.017
Bellotti *et al.*	16	$<8.0\times10^{-4}$

The ^{6}Li case was one of the earliest to be considered. In 1958, Wilkinson[13] set an upper limit of 0.2 eV on $\Gamma_{\alpha d}$, the partial width for α decay. (The state decays radiatively with a total width[14] of 8 eV.) The best limits come from the more recent measurements of Barrette *et al.*[15] and Bellotti *et al.*[16] Table I summarizes the experimental situation. A detailed theoretical analysis is presented elsewhere[17] and shows that $\Gamma_{\alpha d}$ is probably orders of magnitude smaller than even the best of these limits. In our experiment we have improved the limit by three orders of magnitude without seeing a positive signal.

II. EXPERIMENTAL METHOD

The present experiment used a high resolution magnetic spectrometer[21] to detect ^{6}Li produced by radiative capture

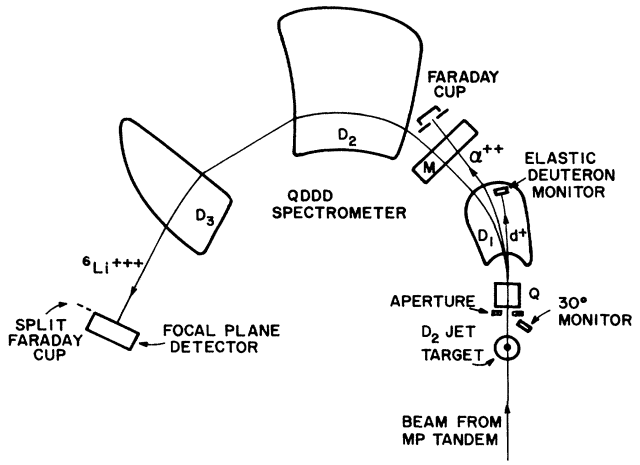

FIG. 1. Schematic diagram showing relative locations of target, QDDD magnet poles, Faraday cup, monitor counters, and focal-plane detector.

in the $^2H(\alpha,\gamma)^6Li$ reaction. With a 6.2-MeV ^4He beam incident on a D_2 gas target, ^6Li nuclei produced at all angles in the center-of-momentum frame recoil forward within a cone of half-angle 0.9° in the laboratory frame. The quadrupole-dipole-dipole-dipole (QDDD) magnetic spectrometer was used at 0° to separate $^6Li^{+++}$ ions from the ^4He beam, which was collected in a Faraday cup at an intermediate point in the spectrometer (see Fig. 1). The D_2 gas target was a supersonic jet providing a target thickness of 1.7 $\mu g/cm^2$. The excellent emittance and stability of the $^4He^{++}$ beam from the Chalk River MP tandem accelerator enabled the beam to be focused through the 5-mm-diameter apertures of the target assembly with a minimum of scattered beam. When combined with the high dispersion of the QDDD spectrometer, this resulted in manageable background rates of scattered ^4He in the focal plane detector, about 2500 per second for 2 μA of beam. Figure 2 shows schematically the relative locations on the focal plane of the important particle groups. It may be seen that intense beam components interfere with all but the triply-charged ^6Li. Singly charged α particles from elastic scattering at 180° have the same rigidity as $^6Li^{+++}$, but their energy is so low that they are not observed in the detector.

To search for the parity-forbidden resonance, the incident beam energy was varied over a range of 9 keV, centered about the expected energy of the resonance as determined by recent measurements[22] of the mass of ^6Li and the excitation energy of the 3.56-MeV level. The absolute calibration of the beam energy was obtained by matching the rigidity of the $^4He^{++}$ beam to that of a 31-keV Tl^+ beam generated in a positive-ion source with an accurately known accelerating potential. The QDDD spectrometer was used for this comparison.

This section will provide detailed descriptions of the D_2 supersonic gas jet target, the QDDD magnetic spectrometer, the focal plane detector and data-acquisition system, the beam-energy scanning system, and the absolute energy calibration.

A. Gas jet target

To provide the maximum ratio of reaction yield to beam-energy loss, pure deuterium must be used as a target, and for good resolution the target must be windowless. Some consideration was given to using a conventional differentially pumped static target, but it appeared that a supersonic jet[23] would provide a more nearly ideal object for the spectrometer, and would allow a larger canal for beam and reaction products.

Pure D_2 gas at atmospheric pressure was cooled to approximately 200 K and supplied to a converging-diverging ("de Laval") nozzle made of glass. (The cooling of the target assembly was incidental to its operation and was intended to reduce backstreaming of oil vapors from mechanical pumps into the target chamber.) Design of the nozzle was empirical. A nozzle with a throat diameter of 0.69 mm, an exit diameter of 1.0 mm, and a throat-to-exit length of 5 mm gave very satisfactory results for D_2 and O_2. The main gas flow entered a 13-mm diameter 20-mm-long receiver pumped directly by a 30-l/s mechanical pump. Three additional stages of differential pumping were provided by Roots pumps, two of 70-l/s and one of a 200-l/s capacity. Each section was isolated from the next by a pair of highly polished 5-mm-diameter aluminum apertures (the aperture nearest the spectrometer was 6 mm to allow the full ^6Li-recoil cone from the target to pass through with some margin). The target head (Fig. 3) was a modular unit 13 cm in diameter that mounted conveniently in the existing target chamber of the spectrometer. The scattering chamber was pumped by a 1500-l/s turbomolecular pump backed by the 200-l/s Roots pump. Under normal operating conditions a target thickness of 1.7 $\mu g/cm^2$ was achieved with a chamber pressure of 6×10^{-4} Torr (ion-gauge reading, uncorrected for D_2 relative to air). Pumping restrictions gave satisfactory pressures in the QDDD and the beam line (5×10^{-6} and

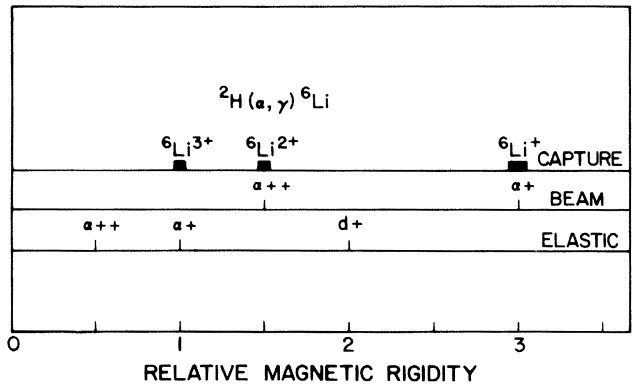

FIG. 2. Relative magnetic rigidity of major particle groups resulting from α bombardment of ^2H. These relationships are independent of beam energy. The widths of the ^6Li (capture) groups are appropriate to a center-of-mass energy of 2 MeV.

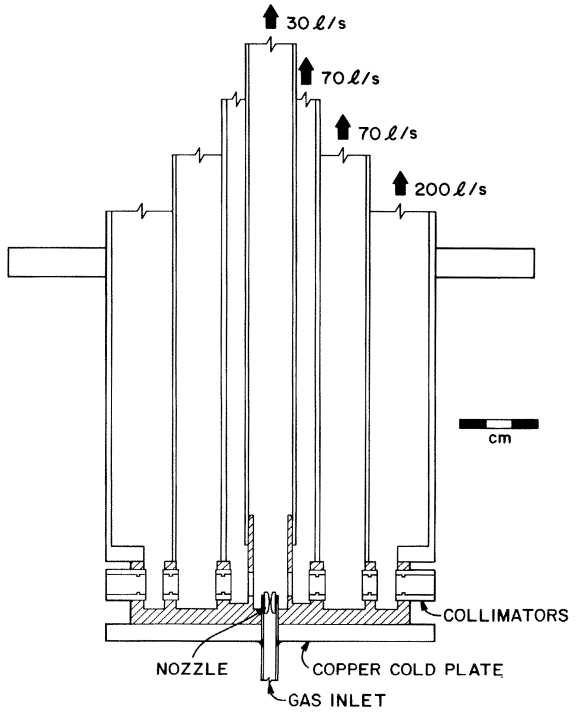

FIG. 3. Cross-sectional view of gas-jet target, showing nozzle and collimator locations.

1×10^{-6} Torr, respectively). Target thicknesses were measured by centering a 6.2-MeV $^4He^{++}$ beam on a split Faraday cup in the focal plane of the QDDD and observing the change in incident energy necessary to recenter the beam when the D_2 jet was turned on.

The deuterium gas was recirculated through an oil vapor trap and one of two interchangeable molecular sieve cryotraps. Gas purity was monitored by observing elastically scattered ^4He in a silicon surface barrier detector mounted in the QDDD target chamber at 30° to the beam. The detector viewed the jet through a 1.5-mm-diameter hole passing through the walls of the target assembly. The gas purity remained high throughout (impurities with $Z \geq 6$ were not observed at the level of 10^{-4} or less). Approximately once every two days the molecular sieve cryotraps were interchanged to maintain gas flow and the out-of-use trap was baked and evacuated.

B. Magnetic spectrometer and beam transport

The Chalk River QDDD magnetic spectrometer[21] has high dispersion, large solid angle, and an intermediate vertical focus after the first dipole that provides a convenient point to intercept all the $^4He^{++}$ beam without interfering with the $^6Li^{+++}$ particles of interest. In addition, internal baffles were installed to prevent scattered beam from reaching the focal plane. The Faraday cup was rectangular (6.2 cm by 1.8 by 1.9 cm deep) and could be inserted radially at a point near the multipole element following the first dipole. A 25-cm-long, 3-cm-high grounded antiscattering shield was attached to the cup to remove degraded and scattered beam.

A 300-mm^2 silicon surface-barrier detector was installed at a point just inside the rear pole face of the first dipole to provide a monitor of ^4He-^2H interactions in the gas target (see Fig. 1). This detector monitored elastically scattered deuterons from the $^2H(\alpha,d)^4He$ reaction at 0°. The effective solid angle of this deuteron monitor detector was measured by determining the number of alpha particles detected from a calibrated ^{241}Am source installed at the center of the QDDD target chamber in place of the D_2 gas jet. The QDDD magnetic field was adjusted so that the 5.48-MeV α^{++} particles would follow the same paths as the 5.56-MeV deuterons. The measured solid angle, 0.160(3) msr, agreed with calculations based on the known focusing properties of the QDDD spectrometer.

To ensure reproducibility in the magnetic field profiles of the QDDD spectrometer and accelerator analyzing magnet, a consistent procedure was used when changing the magnetic fields. The coil currents were increased to a value well above the saturation field of iron and then decreased at a regular rate to the operating point. The magnetic fields in the QDDD were controlled by Rawson-Lush rotating-coil probes interfaced to a microcomputer and to a PDP-10 computer, which controlled the field cycling. Under normal operating conditions the fields were held constant to about 1 part in 10^5 by these probes.

The beam-transport system prior to the spectrometer was carefully adjusted and monitored to minimize scattered beam. Adjustable apertures were installed at points where the beam formed a waist. These apertures were on telescope mounts and could be replaced by a telescope for aligning the beam transport elements and the gas target assembly. After the beam had been optimized at each waist, the apertures were opened to avoid intercepting any beam. Small adjustments of the final few transport elements were occasionally made during the experiment to minimize counting rates of scattered α particles in the focal-plane detector.

To scan the incident energy over the desired range of 9 keV, an independent set of excitation coils in the analyzing magnet was driven with a linear-ramp current waveform. A field-tracking nuclear magnetic resonance (NMR) device was used to monitor the field in the analyzing magnet, and the last three digits of the frequency counter were encoded during data acquisition. In addition, the current in the switching magnet immediately prior to the QDDD was adjusted in synchronism to compensate for the energy variation. However, no attempt was made to sweep other beam-transport elements inasmuch as the energy variation was small and the focus condition implied the absence of first-order variations.

C. Focal plane detector

The focal-plane detector was designed to detect ^6Li ions reliably at a rate of 100 per hour in the presence of α-background rates in the vicinity of 2.5 kHz. The α particles, having generally the same magnetic rigidity as the 4.16-MeV $^6Li^{+++}$ recoils, had an energy of 2.77 MeV. Thus pileup events resulting from the coincidence or near-coincidence of two α particles represented a potentially serious background close to the ^6Li events.

A cross-sectional diagram of the detector is shown in Fig. 4. It is a stopping proportional counter with a ΔE and an E section separated by a ground plane of 8-μm-diameter wires. Two multiplication wires (2.5 μm nickel) in the ΔE section lie below the active volume of the detector, and seven wires in the E region are above the active volume. Thus secondary electrons drift in opposite directions in the two halves of the detector. Pileup events, wherein two particles leave tracks that arrive simultaneously at the ΔE wires, will in general be time resolved at the E wires, and vice versa. Only when the particles arrive at the same time and at the same vertical position will

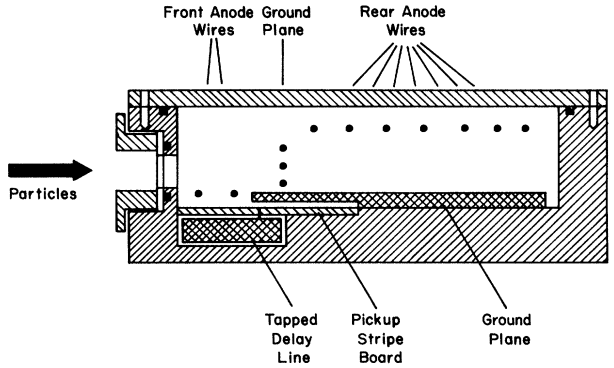

FIG. 4. Cross-sectional view of focal plane detector. The outline is that of the prototype developed at MSU; the larger version used at CRNL differs only in mechanical detail.

they be indistinguishable from a single event. Horizontal readout is by pulses induced on a pickup-stripe board placed beneath the ΔE wires. The stripes are connected to a tapped, continuously wound delay line. Just as with the vertical readout, pulse pairs that may be superimposed at one end of the delay line are generally time resolved at the other end. Thus the only pileup events not identifiable as such are those for which particles arrive at the same time and within the same small area defined by horizontal and vertical position resolutions, about 1 mm in each direction. The readout method provides an effective pulse-pair resolving time of about 100 ps, averaged over the full detector aperture. With this detector, the pileup peak was reduced to the level where it was of no concern, and the main background (at a level of less than 1% of the ^{6}Li events) came from the tail of the single-α peak.

The detector window was aluminized, stretched polypropylene of 140-μg-cm^{-2} thickness, and the gas filling 40 Torr of isobutane. Gas flowed slowly through the detector at a pressure maintained by a servo-controlled needle valve. Operating voltages were typically 700 V on both front and back wire planes. To protect the detector during beam-energy calibrations when the full beam was brought to the focal plane, a flap operated by compressed air was placed over the detector aperture.

D. Data acquisition

Nine-parameter events from the focal plane detector were recorded on magnetic tape and monitored on line by a PDP1 computer. An event consisted of energy signals from each of the ΔE and E wire planes; two time-to-amplitude converter (TAC) signals corresponding to the time difference between the two ends of the delay line and to the time difference between the ΔE and E energy signals (vertical position information); four pulse shape discrimination signals for the E, ΔE, and the two ends of the delay line (to indicate pileup); and finally a word containing the three least significant digits of the NMR-frequency reading for the tandem analyzing magnet. The number of beam-target interactions as a function of incident energy was monitored by recording single-parameter events consisting of the NMR signal triggered by every tenth elastic deuteron detected. To ensure that the particle-identification techniques were correct for ^{6}Li^{+++}, these ions were produced at the appropriate energy via the ^{6}Li(α,^{6}Li)^{4}He reaction with 4.38-MeV α ions incident on a thin ^{6}LiF target placed in front of the jet target.

E. Li detection efficiency

The efficiency for detecting ^{6}Li recoils is dictated entirely by the fraction f^{3+} having charge 3. Measurements of charge-state fractions were made with both solid and gaseous targets. At MSU, α beams of 5.33 and 6.10 MeV bombarded targets of ^{6}LiF on 20-μg/cm^2 carbon backings. Singly, doubly, and triply charged ^{6}Li recoils were observed in an Enge spectrometer at 33.5°. Data were taken both with the ^{6}LiF layer towards the spectrometer and away from it, no difference being observed. At Chalk River a ^{6}Li^{+++} beam was produced and analyzed in the QDDD spectrometer, and its current measured with and without targets in place. (Only the 3^+ charge state was measured in these experiments.) Solid carbon targets of 5 μg/cm^2 and the D_2 jet target at a range of supply pressures were studied. Results of the measurements of f^{3+} are summarized in Fig. 5. There is good agreement between tabulated values[24] and the measurements made on carbon foils with different techniques at MSU and CRNL. The gas-target data, however, show a completely different energy dependence, with f^{3+} remaining near 100% to quite low energies and then dropping rapidly. Some direct comparison measurements were also made wherein carbon foils were placed ahead of the gas jet. These checks confirmed that the gas jet produced high charge states. Measurements as a function of jet-target thickness showed that the gas target was about twice as thick as needed to equilibrate the charge-state distribution. There is some uncertainty as to the charge-state distribution of ^{6}Li recoils produced near the downstream edge of the target, but in the absence of other information we use the thick-target results. At 4.16 MeV, the ^{6}Li energy corresponding to the 3.56-MeV resonance, the triply charged fraction from stripping in D_2, is 0.98(1).

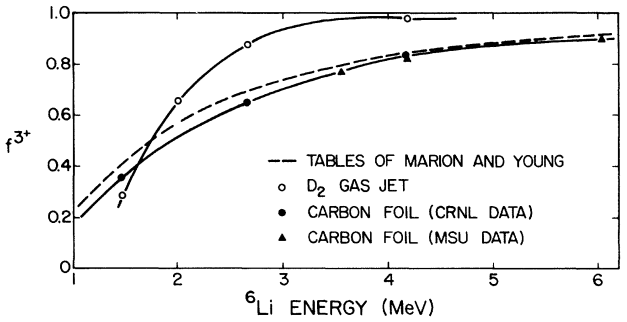

FIG. 5. Fraction of ^{6}Li ions leaving in the 3^+ charge state from the D_2 jet target and from carbon foils. Also shown are data from Marion and Young (Ref. 24).

The only other significant contributor to detection inefficiency was dead time, but since the elastic deuterons used as a normalization (prescaled by a factor 10) were recorded in competition with events from the focal-plane detector, an approximate dead-time correction is automatically made. Because of hardware cuts imposed on the recorded data, raw dead times were only of order 1% in any case.

F. Absolute beam energy calibration

To ensure that the resonance was within the beam energy range of the experiment without use of unduly large scanning ranges, it was required that the beam energy be known with an absolute accuracy of about 2 parts in 10^4; it was also desirable to match the beam energy from one data-acquisition period to the next with an accuracy of 1 part in 10^4. For this purpose, a surface-ionization source[25] was built, which, operating at 30.5 kV, produced Tl^+ ions having the same magnetic rigidity as the 6.24-MeV α^{++} beam particles. By means of a bending magnet 7 m upstream from the spectrometer, either beam could be

brought down the beam line and through the spectrometer to a split Faraday cup at the focal plane. The position and angle of the beams at the entrance to the spectrometer were defined by a 0.5-mm slit in the target chamber and a 3.0-mm spectrometer aperture, so that when each beam was centered on the split Faraday cup, the magnetic rigidities were matched. Because of the thermal nature of the ionization process, the energy of the Tl^+ beam could be determined by measuring the source voltage with a precision voltage divider and voltmeter. These beam energy calibrations were repeated at about three-day intervals during the data-acquisition periods.

The source voltage was provided by a highly regulated low-ripple (<10 ppm rms) DC power supply, whose output voltage was measured by a Julie Research Laboratories KV-50 voltage divider having a dividing ratio of 5000, an absolute accuracy of 0.01%, and a stability rated at better than 15 ppm per year, together with a Fluke 8502A multimeter having a rated accuracy of 0.002% for 90 days. Both instruments were independently calibrated by the Division of Physics of the National Research Council of Canada in Ottawa before the experiment, and the divider was recalibrated after the experiment at the Comtel Standards Laboratory, Detroit, Michigan. From these calibrations a divider ratio of 4999.4(5) was established.

Uncertainties in the beam energy measurement result from voltage divider and voltmeter calibrations, spectrometer aberrations, contact-potential effect, and uncertainties in determining the split-Faraday-cup balance point for the two beams. These effects combine[25] to give an absolute accuracy of 1.6 parts in 10^4 (1.0 keV).

III. RESONANCE YIELD

Since the natural line width of the 0^+, $T=1$ state in ^{6}Li is only 24 eV in the laboratory frame, the resonance line shape for a very thin target is determined principally by beam energy spread and Doppler broadening. These effects combine to give a resonance profile that is closely Gaussian in shape. Thus the resonance cross section may be written

$$\sigma(E)=\sigma_0 \exp\left[-\frac{1}{2}\left[\frac{E-E_R}{\delta}\right]^2\right],$$

where σ_0 is a normalization, E_R is the resonance energy, and δ is a width parameter equal to the quadrature of the beam and Doppler standard widths.

The number of reactions per incident particle (the "yield," Y) for a monoisotopic target whose thickness in energy units is β, is

$$Y=s^{-1}\int_{E-\beta}^{E}\sigma(E')dE',$$

where s is the atomic stopping power. If the target is much thicker than δ, the "thick-target yield" is then

$$y=s^{-1}\sigma_0\delta\sqrt{2\pi}.$$

More generally, the integral is the difference between two error functions, but it resembles a Gaussian:

$$\int_{E-\beta}^{E}\sigma(E')dE'\cong\beta\sigma_0\exp\left[-\frac{1}{2}\left[\frac{E-E_R-\beta/2}{\epsilon}\right]^2\right],$$

where ϵ is given by

$$\epsilon=\left[\delta^2+\tfrac{1}{12}g^2\beta^2\right]^{1/2}.$$

The parameter g ranges from 1 to $[3/(2\ln 2)]^{1/2}$, depending on whether $\beta\ll\delta$ or $\beta\gg\delta$, respectively. Defined in this way, ϵ and g give the Gaussian a FWHM equal to the value obtained by exact evaluation of the integral at the thick- and thin-target limits. For intermediate cases, g must be evaluated numerically, and in the present instance $g=1.13$. The Gaussian approximation becomes exact for thin targets, and even at the thick-target limit it overestimates the height of the yield step by only 7%. In this formulation we neglect both discrete aspects of stopping powers (which lead to complex line shapes) and fluctuations in stopping (which lead to straggling and asymmetrical line shapes). Our interest is mainly in the integral yield, which is not altered by these effects in first order. The error involved in parametrizing the yield by a symmetrical function is assumed to be negligible, as evidenced by the line shape observed in $^{16}O(\alpha,\gamma)^{20}Ne$ (see below).

The relationship between the natural partial width and the thick-target yield is[26]

$$\frac{2J+1}{(2j_1+1)(2j_2+1)}\Gamma_{\text{c.m.}}=\frac{m_2}{m_1+m_2}\frac{2s}{\lambda^2}y,$$

where λ is the center-of-mass wavelength of the incident particle; J, j_1, and j_2 are the spins of the resonance, the projectile, and the target, respectively; m_1 and m_2 are the masses of projectile and target, respectively; and $\Gamma_{\text{c.m.}}$ is the resonance α width in the center of mass (here assumed to be small compared to the total width).

Hence the total yield (resonant plus nonresonant capture) may be written

$$Y_T=s^{-1}\beta\sigma_{\text{NR}}\left\{1+\frac{\lambda^2}{2\sigma_{\text{NR}}\delta 2\pi}\frac{m_1+m_2}{m_2}\frac{2J+1}{(2j_1+1)(2j_2+1)}\Gamma_{\text{c.m.}}\exp\left[-\frac{1}{2}\left[\frac{E-E_R-\beta/2}{\epsilon}\right]^2\right]\right\}, \quad (1)$$

where σ_{NR} is the nonresonant capture cross section. The coefficient of the exponential is the quantity that we extract by fitting the data.

Determination of the parity-forbidden width $\Gamma_{\text{c.m.}}$ ($\equiv\Gamma_{\alpha d}$) thus requires knowledge of the target energy loss β, the resolution width parameter δ, and the nonresonant cross section σ_{NR}. Evaluation of σ_{NR} is made by comparing the total observed ^{6}Li capture rate with the rate for the $^2H(\alpha,d)^4He$ elastic scattering process after correcting for detection efficiencies. The cross section for elastic scattering of deuterons from alphas has been measured by several groups at center-of-mass energies near

2.08 MeV. The data of Galonsky *et al.*[27] extend both above and below this energy and to a scattering angle of 176°. We adopt their value for the center-of-mass differential cross section, 115(7) mb sr^{-1} for the ^{4}He(d,d)^{4}He reaction at 176°, and note that it is entirely consistent with the measurements of Mani and Tarratts,[28] and of Senhouse and Tombrello,[29] when reasonable methods are used to extrapolate to backward angles. With this normalization the nonresonant capture cross section at $E_\alpha = 6.238$ MeV is

$$\sigma_{NR} = 16.0(9) \text{ nb} .$$

The uncertainty is dominated by the uncertainty in the elastic-scattering cross section.

The target energy loss β was determined directly by bringing the 6.24-MeV α beam to a focus on the split Faraday cup in the QDDD focal plane with the gas target turned off and then measuring the change in beam energy needed to restore balance when the target was turned on. The target thickness was found to be 1.65 keV. This corresponds to approximately 1.7 μg cm^{-2}, but it should be noted that our results are independent of the stopping power s.

To determine the energy resolution of the ^{4}He^{++} beam, O_2 gas was used in the target, and the 2^+, $T=1$ resonance[30] in ^{20}Ne was populated via the ^{16}O(α,γ)^{20}Ne reaction at an incident energy of 6.92 MeV. Gamma rays were detected in a pair of 12.5-cm-diameter 15-cm-long NaI(Tl) detectors installed outside the QDDD scattering chamber. The measured line width of 2.30 keV (Fig. 6), the measured target thickness of 0.81 keV, and the natural (Lorentzian) line width of 0.5 keV imply a beam resolution of 1.95 keV FWHM. Doppler broadening, at approximately 0.3 keV, is negligible in this reaction. Doppler broadening is more significant in the ^{2}H(α,γ)^{6}Li reaction, and is complicated by the fact that the gas temperature is rather uncertain because the Mach number for the jet is not well known. Standard gas-dynamic calculations indicate that the effective temperature is a factor of 2 to 3 lower than the supply temperature. We adopt a temperature of 100 K, and find a corresponding Doppler width of 1.2 keV FWHM. The width parameter δ is then 0.97 keV. The results are not very sensitive to the assumed temperature of the jet. A temperature of 300 K would result in a limit on $\Gamma_{\alpha d}$ about 20% worse than the one we report.

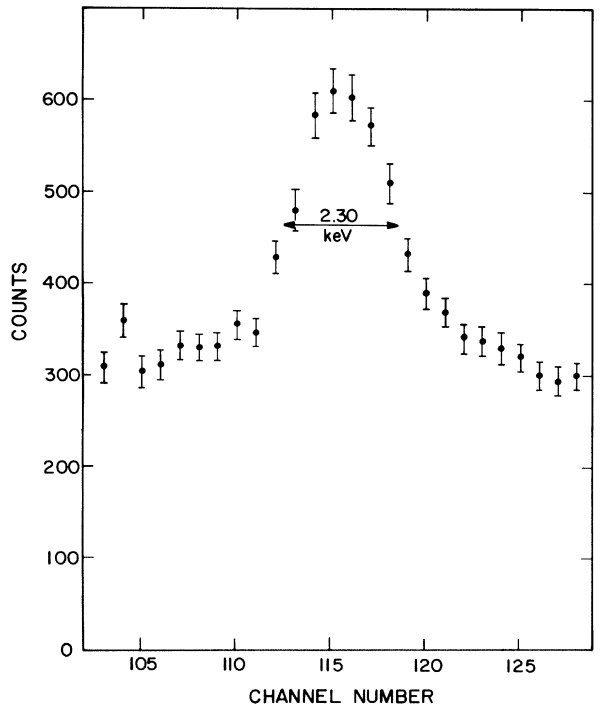

FIG. 6. Resonance in ^{16}O(α,γ)^{20}Ne at 6.92-MeV beam energy.

IV. RESULTS AND ANALYSIS

Analysis of the event-recorded data was carried out on a PDP-10 computer. About 28 000 ^{6}Li events were

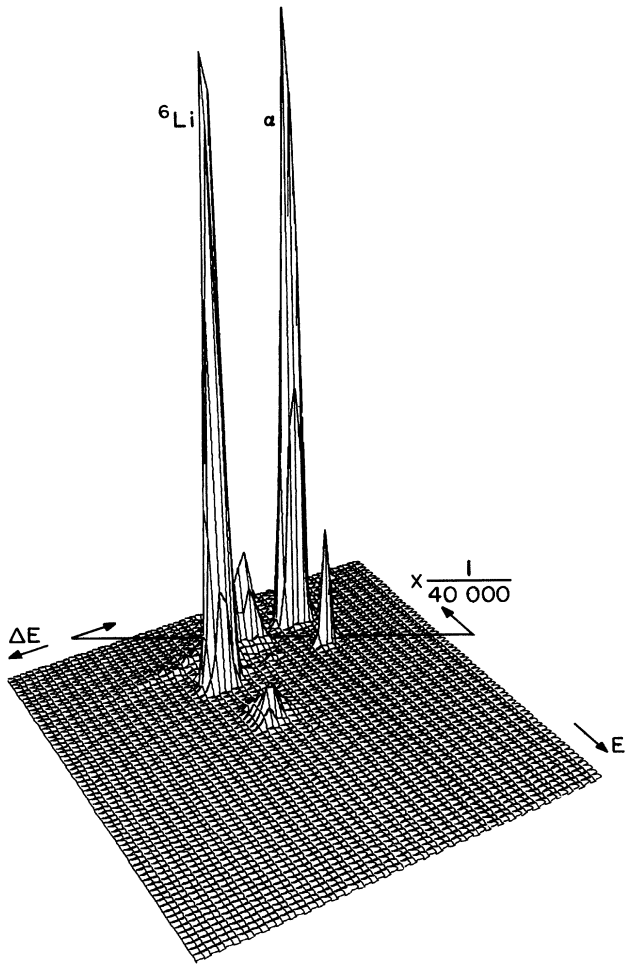

FIG. 7. Plot showing ^{6}Li capture group, scattered-α group (scaled by 40 000) and (foreground) $\alpha+\alpha$ pileup peak. The other two peaks are the tails of the α group cut off by the local scaling factor.

recorded during a ten-day run ("run A"). In addition, an earlier run giving about 4000 events was also analyzed ("run F"). To improve the quality of the spectra, correlations between several of the parameters were removed during the sorting process. Both the E and ΔE energy spectra were corrected for correlations with vertical position, and a sum spectrum of $E+\Delta E$ was formed. The two delay-line pulse-shape spectra were corrected for correlations with horizontal position. The horizontal position spectrum was corrected for its correlation with beam energy.

After correction for the correlation effects, cuts were imposed on the pulse-shape-discrimination and vertical-position spectra, and two-dimensional spectra for ΔE vs total energy were obtained. A typical spectrum is illustrated in Fig. 7. The ^{6}Li events are clearly resolved from the events owing to scattered alpha particles and also from the events near the center of the diagram arising from two alpha particles arriving simultaneously at the detector. With additional cuts on ΔE and E to select ^{6}Li events, a spectrum was obtained (Fig. 8) for the focal plane as derived from the TAC applied to the horizontal delay line. The variation in count rate with focal plane position (^{6}Li momentum) results from the angular distribution of the recoiling gamma rays. The distinctive double-lobed pattern can be described by a direct capture calculation[31] as arising from the predominant $E2$ transition. The asymmetry is a result of $E1$-$E2$ interference. The solid line is derived from such a calculation, as described in Ref. 31.

The small peak near the middle of the distribution arises from a very small ^{6}Li component present in the $^4He^{++}$ beam. The probable origin of this ^{6}Li component is the charge-exchange canal of the ion source, which uses Li. A small number of $^6Li^-$ ions may be formed near the extraction electrode and accelerated to the Van de Graaff terminal. If they emerge from the gas stripper in the 1^+ charge state, they will reach 4.16 MeV at the high-energy end of the accelerator. Loss of another electron, in the residual gas of the beam line before the analyzing magnet, leads to an ion having the same magnetic rigidity as the 6.24-MeV α^{++} beam. These ions can be transported without attenuation to the jet target where they can be stripped to the 3^+ charge state and detected at the QDDD focal plane. (The peak width is representative of overall position resolution in the focal plane.) That this peak in the spectrum arose from a component of the beam was demonstrated subsequent to the accumulation of the majority of the data by the addition of a velocity filter in the beam line in front of the target. The velocity filter completely eliminated the peak. This region of data (two channels) was excluded in subsequent data analysis.

The experimental results on the resonant capture process are, in essence, an excitation function for the

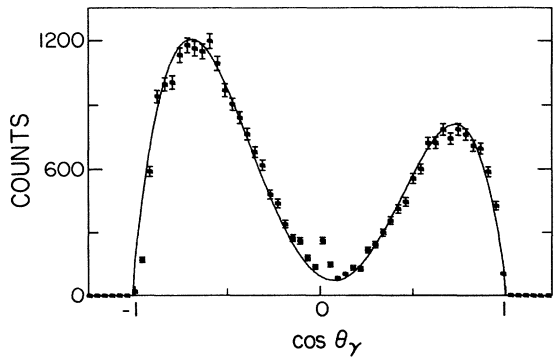

FIG. 8. Momentum distribution of ^{6}Li ions. The momentum varies linearly (to an excellent approximation) as the cosine of the angle between the incident beam and the outgoing photon, θ_γ. The solid curve is a direct-capture calculation in which the $E1$ operator has been renormalized to provide the best agreement with the data. The small peak in the center of the distribution is from a weak ^{6}Li component in the beam (see text).

$^2H(\alpha,\gamma)^6$Li reaction, and it would be straightforward to set limits on the presence of a resonance in the total capture cross section. However, a significant improvement in statistical accuracy can be achieved by noting that angular-distribution data are also available at each beam energy, and that the resonance being sought has spin 0. We may thus search for a resonance in the isotropic component of the angular distribution only, and at the same time constrain the anisotropic components to be nonresonant. Because the angular distribution in this case is highly anisotropic, the extra constraint increases the equivalent statistical accuracy by about 50%. In physical terms, it may readily be observed that the data are very sensitive to the presence of an isotropic component in the region near 90°, where the angular distribution is at a minimum. This extra sensitivity is lost in an analysis that uses only the total number of counts at each energy.

To determine the amplitude of the parity-violating resonance, we searched the two-dimensional spectrum of focal-plane position versus beam energy for a Gaussian-shaped peak (in the energy dimension) that was isotropic in the angular distribution of the γ ray (the angle being determined by the focal plane position). The data were binned into a region of 28 energy channels by 49 position channels. A few channels in two corners of this spectrum were omitted from the fits as counts in these channels were reduced when the momentum distribution moved slightly off the edge of the detector at the extremes of the beam-energy scanning range. The formula fitted to the data was

$$C(E_\alpha,\cos\theta_\gamma)=N_d(E_\alpha)\left\{\sum_{n=0}^{4}a_nP_n(\cos\theta_\gamma)+A\exp\left[-\frac{1}{2}\left[\frac{E_\alpha-E_R-\beta/2}{\epsilon}\right]^2\right]\right\},$$

where E_α is the incident beam energy, θ_γ is the γ-ray angle, $N_d(E_\alpha)$ is the number of deuteron events in the 0° monitor detector, the a_n are coefficients of the Legendre polynomials $P_n(\cos\theta_\gamma)$ (summing through $n=4$ accounts for $E1$ and $E2$ contributions to the reaction and their cross terms), and A is the amplitude of the resonance. The

ratio A/a_0 is the coefficient of the exponential in Eq. (1).

The relation between the incident energy and the corresponding channel number is determined from the Tl^+ ion source calibration, as described above. We neglect the difference in variation with energy of the cross sections for $^2H(\alpha,d)^4He$ and $^2H(\alpha,\gamma)^6Li$, which is about 0.2% across the search range.

The parameters to be varied in fitting the data are A, E_R, a_n, and a gain parameter b that relates focal-plane position to $\cos\theta_\gamma$. This relationship is

$$\cos\theta_\gamma = -\frac{p_0 c}{E_\gamma}\left[D_x^{-1}\Delta x + \tfrac{1}{2}D_x^{-2}(\Delta x)^2 - \frac{1}{2}\left[\frac{E_\gamma}{p_0 c}\right]^2\right],$$

where p_0 is the momentum of the recoiling ^6Li, E_γ is the γ-ray energy (3.563 MeV), D_x is the dispersion[21] of the QDDD (850 cm), and Δx is given in cm by

$$\Delta x = b(\text{channel} - d) .$$

The parameter d can be determined conveniently from the position of the contaminant ^6Li-beam peak in the middle of the angular distribution.

As the number of counts per channel in the two-dimensional spectrum was small (often less than 10, the maximum being 60), it was necessary to use Poisson statistics to determine the best fit to the data. Because it was not feasible to search the entire eight-dimensional parameter space for the best fit, the gain parameter b and preliminary values for the ratios a_1/a_0, a_2/a_0, a_3/a_0, and a_4/a_0 were obtained from a least-squares fit to the two-dimensional spectrum. Then, with $A=0$, the Poisson probability ($\prod \mu^m e^{-\mu}/m!$) was calculated in four two-dimensional spaces: (1) a_0 vs a_1/a_0, (2) a_0 vs a_2/a_0, (3) a_0 vs a_3/a_0, and (4) a_0 vs a_4/a_0, where in each of the four cases the ratios a_i/a_0 not being varied were fixed at the values obtained from the least-squares fit. The best-fit a_i/a_0, for $i=1$–4, obtained were then used as central values for a further Poisson iteration. Two iterations gave a convergent result. Finally, using these four ratios as central values, the four two-dimensional searches were carried out for a grid of a_0, A, and E_R, thus eliminating the effects of possible correlations between the angular distribution and resonance parameters. For the value of a_0 giving maximum probability a probability map in the A vs E_R space was obtained. This map is shown for run A in Fig. 9. If these points are now weighted according to the probability that we expect to find the resonance in a given incident-energy channel (the two-dimensional data alone cannot eliminate the possibility of a large resonance centered just outside the scan range), we can calculate the likelihood function for the parameter A. We use the value 6.2392 MeV for the most probable resonance energy and a standard deviation of 0.0021 MeV. This value represents the expected resonance energy [6.2384(18) MeV] based on the ^6Li mass,[22] corrected for target thickness, with an additional 1.0 keV uncertainty from calibration of the beam energy.[25] The most probable value for $\Gamma_{\alpha d}$ is 0. By numerical integration of the likelihood function, we find that at the 68% confidence level[32]

$$\Gamma_{\alpha d} \le 4.0\times10^{-7} \text{ eV} ,$$

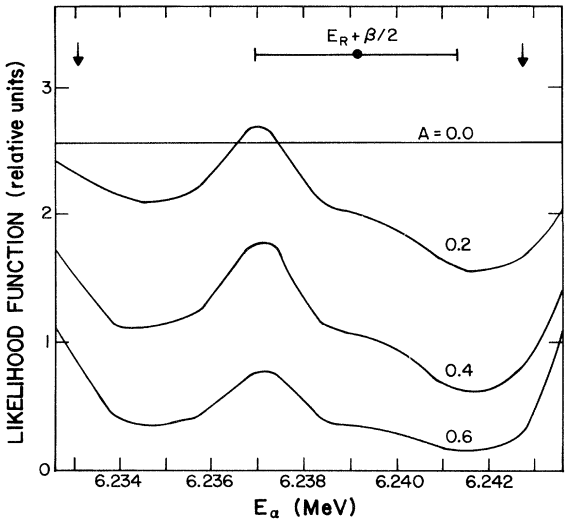

FIG. 9. Calculated values of the likelihood function for a resonance with an amplitude A as indicated on the curves. The arrows indicate the extent of the data.

and at the 90% confidence level

$$\Gamma_{\alpha d} \le 6.5\times10^{-7} \text{ eV} .$$

V. CONCLUSIONS

The limit on $\Gamma_{\alpha d}$ obtained in these experiments is more than a factor of 1000 below that set in previous experiments. Given that a parity- and isospin-allowed $L=1$ decay width for a state at 3.56 MeV is of order 2 MeV, our result sets a limit on the 0^-, $T=0$ amplitude in the 0^+, $T=1$ state of about 6×10^{-7}.

Desplanques, Donoghue, and Holstein[33] (DDH) have presented a quark-model calculation of strengths of weak nucleon-nucleon potentials mediated by the exchange of various mesons. Weak pion exchange is expected to dominate the isovector parity mixing under investigation in the present work—barring fortuitous cancellations, the exchange of heavier mesons can be neglected. It was found by DDH that, within the broad constraints of the quark model, the strength of the weak π-nucleon coupling constant f_π should with high probability lie between 0 and 30 (in units of the "sum-rule" value $g_\pi = 3.8\times10^{-8}$). They suggested a "best" value of about 12, and an analysis[2] of experiments[4,5] in ^{19}F and ^{21}Ne is consistent with this value, although the results depend on very complex nuclear structure calculations[8,9] in the case of ^{21}Ne. Pure isovector parity violation has been sought in two experiments (that are amenable to theoretical interpretation), the capture of polarized neutrons by protons[10] and the circular polarization[12] of γ rays from the 1080-keV state of ^{18}F. Upper limits on f_π of about 40 have been set in the first case and of about 13 in the second.

In the case of ^6Li, interpretation of the α width in terms of f_π requires a structure calculation, which is presented elsewhere.[17] The result of that calculation is

$$\Gamma_{\alpha d} = 9.3\times10^{-11} f_\pi^2 \text{ eV} .$$

Our measurements thus correspond to $f_\pi \leq 66$ (68% C.L.) or $f_\pi \leq 84$ (90% C.L.). (C.L. is confidence level.)

Because the limit set here on f_π is still far above that expected, it is interesting to speculate on ways in which the experiment might be further improved. Simply running longer is unlikely to be fruitful because the sensitivity to f_π increases only as the fourth root of the number of events. Bombarding a helium target with deuterons offers the advantages of higher beam currents, better resolution, and a more favorable stopping power, but the difficulties in detecting capture events are formidable. It should perhaps be stressed that this experiment is at the level where nonresonant capture is observed. This represents a physical, irreducible background in any resonance search. To reach the desired level of sensitivity without greatly improving the resolution would imply a resonance-to-background ratio so small as to raise concern about systematic effects that are probably negligible in the present experiment. Perhaps the best approach is to consider ways in which the resonance might be observed in interference with the nonresonant background through the use of polarized deuterons.

ACKNOWLEDGMENTS

We gratefully acknowledge the contributions of R. A. Warner, who played a key role in the initial development of this experiment, and we thank P. S Miller, K. B. Beard, G. Richter, R. L. Brown, J. C. Hill, N. C. Bray, M. G. Steer, and N. Burn, who provided valuable technical advice and assistance. The operating staff of the Chalk River MP Tandem Accelerator made available beams of superlative quality. This research was supported by the U.S. National Science Foundation through Grant No. PHY-78-22696, by the U.S. Department of Energy, and by the Alfred P. Sloan Foundation through a fellowship to one of us (R.G.H.R.).

*Present address: Physics Division, Los Alamos National Laboratory, Los Alamos, NM 87545.

†Present address: AT&T Bell Laboratories, Murray Hill, NJ 07974.

‡Present address: Department of Physics, Princeton University, Princeton, NJ 08544.

[1]For recent reviews, see, e.g., D. Tadić, Rep. Prog. Phys. 43, 67 (1980); R. G. H. Robertson, in *Proceedings of the International Conference, "Neutrinos 80,"* edited by E. Fiorini (Plenum, New York, 1981), p. 219.

[2]E. D. Earle, A. B. McDonald, E. G. Adelberger, K. A. Snover, H. E. Swanson, R. von Lintig, H. B. Mak, and C. A. Barnes, Nucl. Phys. A396, 221c (1983).

[3]E. G. Adelberger, M. M. Hindi, C. D. Hoyle, H. E. Swanson, R. D. von Lintig, and W. C. Haxton, Phys. Rev. C 27, 2833 (1983).

[4]E. G. Adelberger, H. E. Swanson, M. D. Cooper, J. W. Tape, and T. A. Trainor, Phys. Rev. Lett. 34, 402 (1975); E. G. Adelberger (private communication).

[5]K. A. Snover, R. von Lintig, E. G. Adelberger, H. E. Swanson, T. A. Trainor, A. B. McDonald, E. D. Earle, and C. A. Barnes, Phys. Rev. Lett. 41, 145 (1978); A. B. McDonald (private communication).

[6]J. Ohlert, O. Traudt, and H. Wäffler, Phys. Rev. Lett. 47, 475 (1981).

[7]L. K. Fifield, W. N. Catford, S. H. Chew, E. F. Garman, D. M. Pringle, and K. W. Allen, Nucl. Phys. A394, 1 (1983).

[8]W. C. Haxton, B. F. Gibson, and E. M. Henley, Phys. Rev. Lett. 45, 1677 (1980).

[9]B. A. Brown, W. A. Richter, and N. S. Godwin, Phys. Rev. Lett. 45, 1681 (1980).

[10]J. F. Cavaignac, B. Vignon, and R. Wilson, Phys. Lett. 67B, 148 (1977).

[11]P. G. Bizzetti and A. Perego, Phys. Lett. 64B, 298 (1976).

[12]C. A. Barnes, M. M. Lowry, J. M. Davidson, R. E. Marrs, F. B. Morinigo, B. Chang, E. G. Adelberger, and H. E. Swanson, Phys. Rev. Lett. 40, 840 (1978); G. Ahrens, W. Harfst, J. R. Kass, E. V. Mason, H. Schober, G. Steffens, and H. Waeffler, Nucl. Phys. A390, 486 (1982); A. M. Hernandez and W. W. Daehnick, Phys. Rev. C 25, 2957 (1982).

[13]D. H. Wilkinson, Phys. Rev. 109, 1603 (1958).

[14]F. Ajzenberg-Selove, Nucl. Phys. A320, 1 (1979).

[15]J. Barrette, W. Del Bianco, P. Depommier, S. Kundu, N. Marquardt, and A. Richter, Nucl. Phys. A238, 176 (1975).

[16]E. Bellotti, E. Fiorini, P. Negri, A. Pullia, L. Zanotti, and I. Filosofo, Nuovo Cimento 29A, 106 (1975).

[17]R. G. H. Robertson and B. A. Brown, Phys. Rev. C 28, 443 (1983).

[18]H. Wahl, Ph. D. thesis, University of Hamburg, 1967 (unpublished).

[19]V. K. Rasmussen and C. P. Swann, Phys. Rev. 183, 918 (1969).

[20]K. P. Artemov, V. Z. Goldberg, I. P. Petrov, V. P. Rudakov, and I. N. Serikov, Yad. Fiz. 14, 1105 (1972) [Sov. J. Nucl. Phys. 14, 615 (1972)].

[21]J. C. D. Milton, G. C. Ball, W. G. Davies, A. J. Ferguson, and J. S. Fraser, Atomic Energy of Canada, Ltd. Report AECL-3563, 1970 (unpublished).

[22]R. G. H. Robertson, J. A. Nolen, Jr., T. Chapuran, and R. Vodhanel, Phys. Rev. C 23, 973 (1981).

[23]J. Ulbricht, G. Clausnitzer, and G. Graw, Nucl. Instrum. Methods 102, 93 (1972).

[24]J. B. Marion and F. C. Young, *Nuclear Reaction Analysis, Graphs and Tables* (North-Holland, Amsterdam, 1968), p. 38.

[25]P. Dyer and R. G. H. Robertson, Nucl. Instrum. Methods 189, 351 (1981).

[26]R. H. Spear, Z. E. Switkowski, D. L. Kennedy, and J. C. P. Heggie, Nucl. Phys. A318, 21 (1979).

[27]A. Galonsky, R. A. Douglas, W. Haeberli, M. T. McEllistrem, and H. T. Richards, Phys. Rev. 98, 586 (1955).

[28]G. S. Mani and A. Tarratts, Nucl. Phys. A107, 624 (1968).

[29]L. S. Senhouse and T. A. Tombrello, Nucl. Phys. 57, 624 (1964).

[30]F. Ajzenberg-Selove, Nucl. Phys. A392, 1 (1983).

[31]R. G. H. Robertson, P. Dyer, R. A. Warner, R. C. Melin, T. J. Bowles, A. B. McDonald, G. C. Ball, W. G. Davies, and E. D. Earle, Phys. Rev. Lett. 47, 1867 (1981).

[32]A similar analysis of the shorter run (run F) gave $\Gamma_{\alpha d} \leq 1.7 \times 10^{-6}$ eV (68% C.L.) and 2.8×10^{-6} eV (90% C.L.).

[33]B. Desplanques, J. F. Donoghue, and B. R. Holstein, Ann. Phys. (N.Y.) 124, 449 (1980).